Journal of the International Neuropsychological Society (2016), **22**, 105–119.
Copyright © INS. Published by Cambridge University Press, 2016.
doi:10.1017/S1355617716000060

CRITICAL REVIEW

Modern Methods for Interrogating the Human Connectome

INS is approved by the American Psychological Association to sponsor Continuing Education for psychologists. INS maintains responsibility for this program and its content.

Mark J. Lowe,[1] Ken E. Sakaie,[1] Erik B. Beall,[1] Vince D. Calhoun,[2,3] David A. Bridwell,[2,3] Mikail Rubinov,[4] AND Stephen M. Rao[5]

[1]Imaging Institute, Cleveland Clinic, Cleveland, Ohio
[2]The Mind Research Network, Albuquerque, New Mexico
[3]Department of ECE, University of New Mexico, Albuquerque, New Mexico
[4]Department of Psychiatry, University of Cambridge, Cambridge, United Kingdom
[5]Neurological Institute, Cleveland Clinic, Cleveland, Ohio

(RECEIVED December 18, 2015; FINAL REVISION January 20, 2016; ACCEPTED January 20, 2016)

Abstract

Objectives: Connectionist theories of brain function took hold with the seminal contributions of Norman Geschwind a half century ago. Modern neuroimaging techniques have expanded the scientific interest in the study of brain connectivity to include the intact as well as disordered brain. **Methods:** In this review, we describe the most common techniques used to measure functional and structural connectivity, including resting state functional MRI, diffusion MRI, and electroencephalography and magnetoencephalography coherence. We also review the most common analytical approaches used for examining brain interconnectivity associated with these various imaging methods. **Results:** This review presents a critical analysis of the assumptions, as well as methodological limitations, of each imaging and analysis approach. **Conclusions:** The overall goal of this review is to provide the reader with an introduction to evaluating the scientific methods underlying investigations that probe the human connectome. (*JINS*, 2016, *22*, 105–119)

Keywords: Human connectome, Resting state fMRI, Diffusion MRI, EEG/MEG coherence, Complex network analysis, Independent components analysis

INTRODUCTION

In "Disconnexion syndromes in animals and man" published 50 years ago, Norman Geschwind (1965a, 1965b) explicated how disparate brain regions communicate by observing the brain disorders of patients with focal lesions. His discovery of disconnection syndromes provided inspiration for contemporary connectionist theories of brain function. Today, modern neuroimaging techniques have enabled the study of both functional and structural connectivity in the intact as well as disordered brain.

The purpose of the current study is to introduce the reader to the modern imaging techniques used to measure functional and structural connectivity, including resting state functional MRI (rs-fMRI), diffusion MRI (dMRI), and electroencephalography and magnetoencephalography (EEG/MEG) coherence. The second section of the study will emphasize the analytical approaches and assumptions, as well as the limitations, associated with these various methods for examining brain interconnectivity.

Correspondence and reprint requests to: Stephen M. Rao, Schey Center for Cognitive Neuroimaging, Neurological Institute, Cleveland Clinic, 9500 Euclid Avenue/U10, Cleveland, OH 44195. E-mail: raos2@ccf.org

APPROACHES TO MEASURING BRAIN CONNECTIVITY

rs-fMRI

Functional connectivity is a descriptive measure for temporal correlations observed between spatially distinct brain regions (Friston, Frith, Liddle, & Frackowiak, 1993; Strother et al., 1995). One such technique for studying functional connectivity, rs-fMRI, involves the acquisition of MRI data with the subject performing no specific task (Biswal, Hudetz, Yetkin, Haughton, & Hyde, 1997; Biswal, Van Kylen, & Hyde, 1997; Biswal, Yetkin, Haughton, & Hyde, 1995; Lowe, Rutecki, Woodard, Turski, & Sorenson, 1997; Peltier & Noll, 2002; Quigley et al., 2003). The method is based on

https://doi.org/10.1017/S1355617716000060 Published online by Cambridge University Press

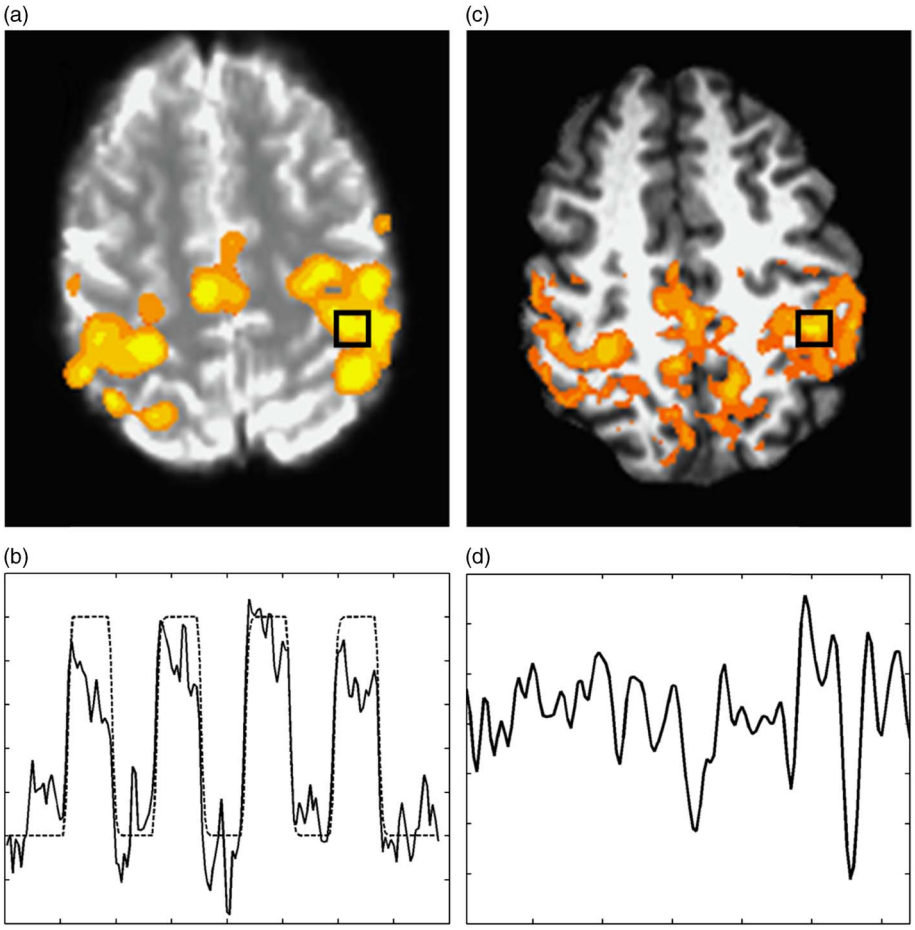


Fig. 1. a: Bilateral finger tapping task activation student's *t* score, thresholded, and overlaid on BOLD-weighted EPI, the black box indicates the maximum activated region, (b) mean timeseries of the black box region in (a) superposed on the task timing (high regions are periods of finger tapping), (c) whole-brain false color map overlaid on high resolution anatomy (overlay indicates regions of high correlation to the region defined by the black box), and (d) timeseries of spontaneous BOLD fluctuations in the boxed region.

the observation that low frequency (<0.1 Hz) spontaneous blood oxygen level dependent (BOLD) fluctuations appear to be temporally synchronous across spatially distinct brain regions, suggesting a pattern of neural connectivity within brain systems (an example involving the motor system is shown in Figure 1).

Spontaneous low-frequency oscillations have been observed in the regional cerebral blood flow and oxygenation of animals and humans using many different techniques, including laser Doppler flow (Golanov, Yamamoto, & Resi, 1994; Hudetz, Smith, Lee, Bosnjak, & Kampine, 1995), fluororeflectometry (Dora & Kovach, 1981; Vern, Schuette, Leheta, Juel, & Radulovacki, 1988), fluorescence video microscopy (Biswal & Hudetz, 1996), polarographic measurement of brain tissue (Cooper, Crow, Walter, & Winter, 1966; Halsey & McFarland, 1974; Moskalenko, 1980), and near infrared spectroscopy (Obrig et al., 2000).

In a series of seminal studies, Biswal et al. (Biswal & Hudetz, 1996; Biswal, Hudetz, et al., 1997; Biswal, Van Kylen, et al., 1997; Biswal et al., 1995) showed that BOLD weighted MRI timeseries data contain spontaneous low-frequency fluctuations that are highly correlated between the right and left primary motor cortex while subjects are at rest. BOLD-weighted MRI allows the monitoring of hemodynamic fluctuations across the entire brain, allowing the study of low-frequency fluctuations over larger distances compared to those of optical studies. This led to many observations of synchronous fluctuations in this frequency domain in MRI timeseries acquisitions. These correlations are present between many different regions of cerebral cortex, which are part of distributed neuronal networks involved in common tasks. This synchrony has been shown to depend on the state of the brain (Lowe, Dzemidzic, Lurito, Mathews, & Phillips, 2000).

Figure 1 shows the results of two typical resting-state fMRI studies of the cortical motor regions of the brain. The false color overlay shows regions of high temporal correlation to the very low frequency fluctuations in the left hemisphere primary motor area (black square) while subjects were resting. It is clear that the regions of highest correlation are the homologous regions in the contralateral hemisphere, as well as the medial motor regions. The source of these temporally correlated fluctuations is unknown, but is currently an area of active investigation. Biswal et al. showed that the correlations

https://doi.org/10.1017/S1355617716000060 Published online by Cambridge University Press

between homologous brain regions are reversibly diminished under hypercapnia, indicating that the effect is blood-flow modulated, similar to BOLD contrast (Biswal, Hudetz, et al., 1997). Furthermore, as is demonstrated by Figure 1, regions of connectivity are not confined to a single vascular distribution. In a subsequent study, Biswal et al. demonstrated that the correlation patterns from BOLD-weighted MRI data were much more similar to task-activated regions from fMRI than the correlations from strictly flow-weighted data (Biswal, Van Kylen, et al., 1997). The combined findings suggested that the BOLD fluctuations represent hemodynamic changes secondary to neural activity.

The precise physiological mechanisms that underlie the high correlations between functionally related brain regions are unclear. However, recent studies have shed light on the neural basis of the spatiotemporal correlations in BOLD fluctuations. These studies have provided direct evidence for neuronal signaling at or below 0.1 Hz and for the notion that spontaneous neuronal activity can reflect functional neural connectivity in the brain. Evidence for an electrophysiological basis for neuronal signaling at 0.1 Hz and below has come from an electrophysiological study conducted in nonhuman primates (Leopold, Murayama, & Logothetis, 2003). These investigators showed that coherent fluctuations in the band-limited field potentials from neurons exist over long time scales (>10 s) and large distances (>25 mm). The band-limited potential, as defined by Leopold et al., is a measure of amplitude modulations of the power of the field potential fluctuations. The same investigators had previously shown that variations in local field potential of neurons correlates well with the BOLD signal (Logothetis, 2002; Logothetis, Pauls, Augath, Trinath, & Oeltermann, 2001). Thus, this report (Leopold et al., 2003) constitutes possible direct observation of a neuronal source of the observed low-frequency BOLD fluctuations.

Support for the notion that spontaneous neuronal activity can reflect functional connectivity came from a study of cat visual cortex using voltage sensitive dye (Kenet, Bibitchkov, Tsodyks, Grinvald, & Arieli, 2003). These investigators observed surprisingly coherent spatial patterns in spontaneous firing with no retinal input. Some of the observed patterns were identical to the cortical activation patterns observed in response to stimuli designed to activate the exposed region of cortex. The authors concluded that the spontaneous dynamically switching cortical states indicate that spontaneous neuronal behavior can reflect functional connectivity within the brain.

An additional study, which performed simultaneous EEG and fMRI in resting subjects, related spontaneous brain activity and functional connectivity (Laufs et al., 2003). The correlation between EEG power in various bands was mapped voxel-by-voxel to the spontaneous BOLD fluctuations. The power observed in the alpha band of the EEG data strongly correlated (inversely) to a broad network of brain regions typically associated with attentional and related cognitive processes. Additionally, positive correlations were observed between power in the beta band and BOLD fluctuations in retrosplenial, tempo-parietal, and dorsomedial prefrontal cortices. The relationship between spontaneous BOLD fluctuations and EEG power in different networks at different bands presents additional evidence to suggest that, during rest, there exist separable networks of brain regions with correlated BOLD fluctuations.

One discovery that has had major implications for the widespread adoption of rs-fMRI as a measure of functional connectivity involved the work of Raichle and colleagues (Gusnard, Akbudak, Shulman, & Raichle, 2001; Raichle et al., 2001). Using quantitative positron emission tomography, they demonstrated the existence of a network of regions that consistently showed higher activity than other brain regions during the resting state. They referred to these regions as the "default mode network" (DMN). Many of these areas (posterior cingulate cortex and precuneus, medial prefrontal cortex, and angular gyrus) also showed significant deactivation during performance of specific tasks. This led to the basic postulate that the brain has a default mode of activity and performance of tasks interrupts this mode. Greicius, Krasnow, Reiss, and Menon (2003) provided MRI support for the Raichle et al. hypothesis by showing that two of the DMN regions (ventral anterior cingulate and posterior cingulate cortices) showed significant low-frequency BOLD correlations during rest.

Furthermore, they showed that, during execution of a cognitive task, the regions known to be involved in task performance showed inverse correlations with the posterior cingulate region. The DMN is now one of the most commonly studied resting state networks in the literature. In addition to the DMN, a very large number of additional brain networks have been identified. Cordes et al. (2000) published one of the first studies to identify multiple functional networks using rs-fMRI. Since then, visual, motor, auditory, attention, and language networks, to name just a few, have been identified in the resting brain.

rs-fMRI is now the predominant method for examining functional connectivity in humans due to the ease of acquiring the data and the generality of the analyses that can be performed on these data. It is important to realize that real-world BOLD data contain various non-neuronal sources of spatiotemporal correlations that are artifactual. To draw proper conclusions, either the data must be corrected to remove these confounds or the analysis must take these confounds into account. This is accomplished either by modeling, regressing and subtracting the projected confound from the data or by including the modeled confound in the connectivity regression analysis.

Furthermore, additional data processing is used before connectivity analysis, including spatial filtering, temporal filtering, and spatial normalization. The choice of processing can have a dramatic effect on the analysis results and some processing methods that were popular in the past have been demonstrated to be associated with bias in the analysis. We note that artifact correction in fMRI and rs-fMRI data is the subject of a large body of literature. The intent of this review is to describe in general terms the most common artifacts with

https://doi.org/10.1017/S1355617716000060 Published online by Cambridge University Press

some basic approaches to correction. In the following paragraphs, we review analytical techniques that are necessary to remove artifacts and typical filtering techniques used to enhance the signal-to-noise ratio of the connectivity signature. Most common fMRI data analysis packages, such as AFNI, FSL, and SPM, include such correction methods.

Motion artifact

Head motion artifact is the most prevalent and difficult artifact because it is difficult to characterize and introduces non-neuronal spatiotemporal correlations. The oldest and most commonly used method to account for head motion is volumetric realignment. It is well known, however, that this does not entirely eliminate artifact. Various regression-based, or "second-order," motion correction methods are used to reduce the residual covariance between the estimated head motion and the BOLD signals (Beall & Lowe, 2014; Bullmore et al., 1999). The second-order motion correction methods vary dramatically in implementation from simple regression of the volumetric motion parameters to models based on voxel-specific motion parameter regression (e.g., motion of each voxel is calculated from the motion parameters).

This still leaves considerable artifact, resulting in more contemporary approaches to minimize the effects of residual motion; for a recent review, see (Power, Schlaggar, & Petersen, 2015). One popular approach involves censoring, that is, rejecting epochs of data surrounding large motions (Power et al., 2012). This has recently been called into question due to the lack of accurate motion metrics (Beall & Lowe, 2014), an issue that applies to all current approaches to motion correction that use volumetric rather than slice-wise estimates of motion. Since fMRI is acquired one brain slice at a time, motion that begins partway through the acquisition of a brain volume will be confined to a subset of slices. Motion metrics based on the local motion of each acquired slice (Beall & Lowe, 2014) have demonstrated promise in correcting motion artifact in rs-fMRI data. Another approach that does not rely on estimation of motion parameters is ICA-AROMA, which uses independent components analysis (ICA) to identify and remove motion-related components (Pruim, Mennes, Buitelaar, & Beckmann, 2015). A more detailed discussion of ICA is presented below in the analysis section.

Physiologic noise

Noise from heart and breathing cycles produces a spatially varying bias in the connectivity patterns and can generally reduce the specificity of network identification. The effect is highly variable across subjects and even sessions due to the variable overlap between the sampling frequency and the aliased physiologic cycles (Cordes, Nandy, Schafer, & Wager, 2014). Consequently, because physiologic rates can vary between populations and states, physiologic noise can result in subtle bias in group analyses, whether using hypothesis-based or data-driven techniques (Beall & Lowe, 2010). The ideal correction would be to model the exact physiologic signal and regress it from the data. However, the exact nature of the artifact induced by a breath or heartbeat is not accurately known and varies across the brain. The current gold-standard for correction is regression of a Fourier series expansion of the physiologic phases (Glover, Li, & Ress, 2000; Hudetz et al., 1995), where the physiologic phases are obtained from monitored pulse and respiration signals synchronized to the acquisition. In many situations, it is difficult to monitor heart and respiration rates. In these cases, it is possible to derive the physiologic traces from the data itself using ICA (Beall & Lowe, 2007; Perlbarg et al., 2007).

Spatiotemporal filtering

Spatial filtering is used to increase signal to noise ratio (Lowe & Sorenson, 1997) and to account for across subject variability in spatial localization of function when performing between group analyses. The problem of cross-subject variability can also be dealt with using subject-specific ROIs for ROI-based analyses or using nonlinear transformations (Cox, 1996). Temporal filtering of resting state data can increase the signal-to-noise ratio of the rs-fMRI effect. The low-frequency BOLD effect underlying functional connectivity is believed to occur at frequencies of approximately 0.1 Hz (the low-frequency cutoff used in literature ranges from 0.08 to 0.12 Hz); therefore, a low-pass temporal filter is often used before analysis. This is based on the fact that the hemodynamic response of the BOLD effect has a very steep cutoff around 0.1 Hz. Thus, any BOLD-derived signal should be slower than 0.1 Hz. This was confirmed in a study published in 2001 (Cordes et al., 2001) and has also been observed in combined electrophysiologic and BOLD studies (Laufs et al., 2003). Higher-frequency connectivity effects have been reported in the literature, but their source is unclear (Boubela et al., 2013; Kalcher et al., 2014).

Detrending

Finally, since its inception, BOLD weighted timeseries data have been observed to have linear trends (Lowe & Russell, 1999). These trends are easy to address by simply regressing a linear (or higher) polynomial fit from the timeseries at each voxel.

dMRI

Diffusion MRI (dMRI) is unique in its ability to map, *in vivo,* the axonal connections that convey neuronal signals. As the other methods described in this article characterize correlations of neuronal activity, dMRI provides complementary information. While individual axons are too small to be resolved by dMRI, large bundles of axons such as the corpus callosum and arcuate fasciculus can be mapped across the entire brain. Analysis of these bundles, also known as fiber tracts or white matter fascicles, is used to assess structural connectivity. We will sketch the basic workings of structural

https://doi.org/10.1017/S1355617716000060 Published online by Cambridge University Press

connectivity analysis and highlight important caveats. Comprehensive reviews are available for further details (Johansen-Berg & Behrens, 2009; Jones, 2010; Tournier, Mori, & Leemans, 2011).

dMRI measures the ease with which water moves. With appropriate mathematical modeling, an intriguing host of information can be inferred about cellular properties from dMRI data. As water moves more easily along white matter fascicles than across, dMRI can be used to infer virtual dissections of entire fasciculi throughout the brain (Catani, Howard, Pajevic, & Jones, 2002). Furthermore, microstructural features such as cell dimension and shapes can, in principle, be measured (Stanisz, Szafer, Wright, & Henkelman, 1997). These two features of tissue, orientation and structure, are central to structural connectivity analysis. Disconnection may be related to abnormal fascicle arrangements or injury to fascicles as reflected by abnormal microstructure. However, dMRI also has fundamental limitations. This imaging method cannot indicate the polarity of axonal connections, that is, the direction of neural signals. Measures of tissue microstructure also depend heavily on the model assumptions. The measures of orientation and structure therefore lack the specificity of histological stains.

Analysis of structural connectivity is a multi-step process. First, a dMRI *acquisition* provides multiple images, each with a different degree of diffusion-related contrast. In diffusion tensor imaging (DTI) (Basser, Mattiello, & LeBihan, 1994), for example, at least seven different image volumes must be acquired. Second, a *model* synthesizes the set of images to yield measures of tissue orientation and structure on a voxel-by-voxel basis. In DTI, fiber bundles align along the principal axis of the diffusion tensor. Demyelination and axonal loss correlate with the degree of diffusivity perpendicular to and parallel to the principal axis, respectively (Song et al., 2003). Third, *tractography* (Mori, Crain, Chacko, & van Zijl, 1999) takes the orientation information from each voxel and generates streamlines that represent long-range axonal connections between cortical regions. Finally, *structural connectivity* among different cortical regions can be assessed by counting the number of streamlines of a given pair of regions (Hagmann et al., 2007).

The basic sketch of steps outlined above provides a framework for understanding the enormous literature describing current research. First, dMRI acquisitions place strong demands on imaging hardware due to the duration of the scan, strong diffusion-weighting gradients and echo-planar imaging readout used to limit the duration of the scan. Quality control must be implemented to ensure that the imaging data are not corrupted by artifact (Oguz et al., 2014; Tournier et al., 2011). Unfortunately, erroneous conclusions may result entirely from image artifacts. The strong gradients induce strong vibrations that can shake electronic components that may be loose on the MR scanner, leading to spikes and increased levels of noise. If, for example, the spikes occur during the latter half of a longitudinal study, an increase in variance may be detected that results entirely from image artifact.

Cardiac gating has been recommended to avoid pulsatility artifact, particularly in periventricular and brain stem regions (Skare & Andersson, 2001). A fingertip pulse plethysmograph is typically used. Such triggering, however, may fail among patients with compromised circulation to the extremities. One inherently difficult problem is motion. dMRI is, by design, sensitive to the motion of water. This sensitivity makes dMRI particularly susceptible to large amounts of head motion. If one group of subjects moves more than another (e.g., patient group greater than control subjects), artifactual between group differences may be detected (Yendiki, Koldewyn, Kakunoori, Kanwisher, & Fischl, 2013).

Among *models*, the diffusion tensor (Basser et al., 1994) is most widely used. As the model requires only six diffusion-weighted image volumes and one image without diffusion weighting, the acquisition time can be as short as 1 min. However, at least 30 diffusion-weighted image volumes are recommended to limit within subject noise in diffusivity measurements (Jones, 2004). From the tensor, one can derive several scalar summary parameters that can be used to assess tissue on a voxel-by-voxel basis. The principal eigenvector of the tensor can be associated with the orientation of white matter fibers in a voxel. Diffusivity along the principal eigenvector, called longitudinal or axial diffusivity, can correlate with axonal fragmentation. Diffusivity perpendicular to the principal eigenvector, called transverse or radial diffusivity, can correlate with demyelination. However, such interpretation depends highly on the injury or disease (Budde et al., 2007) and breaks down at locations with crossing fibers (Wheeler-Kingshott & Cercignani, 2009). The variance among diffusivities is described by fractional anisotropy (FA). Reduced FA is typically interpreted as reduced tissue integrity, but has been found to behave counter to expectations in the presence of crossing fibers (Douaud et al., 2011).

The limitations of the tensor model have stimulated a plethora of alternative models (Assemlal, Tschumperle, Brun, & Siddiqi, 2011) to more accurately capture the complexity of tissue structure. Crossing fibers have received much attention because modeling enables tractography of a wider variety of white matter fascicles than is otherwise possible (Behrens, Berg, Jbabdi, Rushworth, & Woolrich, 2007). More recent work aims to quantify cellular properties such as axon diameters (Assaf, Blumenfeld-Katzir, Yovel, & Basser, 2008) and gliosis (Wang et al., 2011). These models require more extensive and demanding image acquisitions than the diffusion tensor model, resulting in long scans and more stringent hardware requirements. Computation time to fit the models can also be problematically long. The comparison of these models against quantitative histology (Barazany, Basser, & Assaf, 2009; Wang et al., 2011) is more limited than for the diffusion tensor, hampering interpretation.

Tractography essentially works by connecting principal eigenvectors from diffusion tensors of contiguous voxels (Basser, Pajevic, Pierpaoli, Duda, & Aldroubi, 2000; Conturo et al., 1999; Mori, Crain, Chacko, & van Zijl, 1999), resulting in three-dimensional maps of white matter fascicles

https://doi.org/10.1017/S1355617716000060 Published online by Cambridge University Press

(Catani et al., 2002). By accounting for crossing fibers, otherwise occult fascicles can be identified (Behrens et al., 2007). Tractography has been used to investigate Wallerian degeneration. Pierpaoli et al. (2001) showed that white matter connected to, but distal from, an infarct demonstrated abnormal diffusivity consistent with injury. Furthermore, measures of tissue integrity along specific fiber pathways can correlate with functional disability (Lowe et al., 2006) and with resting-state connectivity (Lowe et al., 2008, 2014).

EEG/MEG Coherence

Cortical electrical or magnetic fluctuations can be measured noninvasively with EEG or MEG sensors placed on or above the scalp, respectively. EEG and MEG are important tools for functional connectivity analysis since they provide a direct measure of cortical synaptic activity with high temporal resolution. Additionally, EEG and MEG provide *complementary* measures of functional connectivity, as EEG is preferentially sensitive to radially oriented cortical sources and MEG is sensitive to tangential sources (Cohen & Cuffin, 1983).

The functional connectivity of different cortical regions is often examined in the context of amplitude and phase similarities between signals derived from multiple EEG or MEG sensors. These similarities can be quantified statistically using *coherence*, that is, the squared cross spectrum between two signals normalized by the power spectrum of each signal (Bendat & Piersol, 2000). Conceptually, coherence represents the ratio of the squared covariance of two signals and the variance of each signal, that is, a squared correlation coefficient, providing a measure of the percentage of variance within a signal accounted for by a linear transformation of another signal (Nunez & Srinivasan, 2006). Increases in coherence between signals derived from EEG or MEG sensors may arise due to distributed cortical interactions, revealing functionally connected brain networks that emerge at the time scales of perceptual and cognitive events (Buzsaki, 2006; Engel, Fries, & Singer, 2001).

Within EEG or MEG multi-sensor recordings, it is important to consider whether coherence results from genuine cortical interrelationships or whether it results due to sensor pairs measuring activity from common sources. EEG potentials are spatially smeared by the volume conduction properties of the head, resulting in inflated coherence between EEG sensors within ~10 cm (Srinivasan, Winter, Ding, & Nunez, 2007). MEG signals are unaltered by volume conduction, but measure from common sources due to magnetic field spread (Brookes et al., 2011). These issues are attenuated when spatial filtering and source modeling approaches are applied to estimate the distribution of cortical source potentials that contribute to MEG and EEG sensor measurements (for reviews, see Michel et al., 2004; Schoffelen & Gross, 2009). These approaches may complement each other in functional connectivity analysis, revealing coherent patterns that emerge at different spatial scales and source orientations (Nunez et al., 1999, 1997).

ANALYTICAL APPROACHES TO FUNCTIONAL AND STRUCTURAL CONNECTIVITY

Seed-Based Analyses

The earliest observations of resting-state functional connectivity were made using what is now termed seed-based correlation (Biswal et al., 1995; Lowe, Mock, & Sorenson, 1998). These were serendipitous observations made while studying the noise characteristics of BOLD-weighted MRI timeseries data. Model-based methods, which provide more statistical power and cleaner hypothesis testing, are still very limited to this day due to the fact that there is no "signal" that characterizes the connectivity signature in resting state data, unlike activation-based fMRI. Seed-based correlation analysis remains a very popular technique for analyzing rs-fMRI data. The approach allows the investigator to interrogate the spatial regions of the brain that have a significant temporal correlation to the spontaneous BOLD fluctuations in a pre-specified seed region. In this section, we review typical analysis issues associated with performing seed based analysis of BOLD-weighted MRI timeseries data obtained during the resting state.

Seed-based correlation requires the selection of a seed region, whose connectivity to the rest of the brain is of interest. This is best done with activation-based fMRI using a task related to the function of interest. For example, connectivity related to hand motor function can be examined by acquiring both a resting state scan and a functional hand motor task activation scan (Lowe et al., 1998). The functional scan is used to localize function in the primary motor cortex and a seed region is determined from an activation map (see Figure 1). The mean timeseries in the resting state data averaged over several voxels around the seed region is used to estimate the spontaneous fluctuations in that region.

The use of anatomic localization alone has been shown to be problematic at providing reliable resting state networks (Cole, Smith, & Beckmann, 2010). However, there have been many studies of resting state networks that have been done using anatomic localization, most notably studies of the default mode network (Greicius et al., 2003). The problem is related to that described above when discussing group analyses. Spatial variation in the localization of function can vary considerable across subjects, especially in cortical regions. As with group voxel-level analyses, this is typically addressed by using spatial smoothing. A data-driven method was recently introduced to combine anatomic localization with functional information present in the resting data itself to refine the seed location to improve the robustness of network identification (Lowe et al., 2014). This obviates the need for spatial smoothing.

There are three types of seed-based analyses that are common in the literature: (1) simple Pearson correlation of the seed-derived timeseries with all voxels in the brain, (2) frequency domain analysis of all voxels compared to seed-derived timeseries (Yang et al., 2007), and (3) inter-regional connectivity analyses to determine local interconnectivity

https://doi.org/10.1017/S1355617716000060 Published online by Cambridge University Press

(Zang, Jiang, Lu, He, & Tian, 2004). The first is the most common technique and will be described briefly here. The other methods are beyond the scope of this brief introduction to seed-based connectivity analyses and are mentioned for completeness.

Pearson correlation analysis involves calculating the normalized projection of a reference vector (i.e., seed voxel-derived timeseries) with another vector (i.e., timeseries from any give voxel). It can be expressed as:

$$cc(\vec{x}) = \frac{\vec{x} \cdot \vec{x}_{ref}}{\vec{x}_{ref} \cdot \vec{x}_{ref}}$$

where $\vec{x}$ is the timeseries at a given voxel and $\vec{x}_{ref}$ is the timeseries from the reference, or seed, region. A whole-brain map of this correlation can be produced. A threshold can be applied based on a desired false positive rate and rendered onto high resolution anatomy for display purposes (see Figure 1). Note that the Pearson correlation coefficient has an algebraic relationship to a Student's t (Press, Teukolsky, Vetterling, & Flannery, 1993). Correlation coefficients are intuitive for assessing the level of alignment of the signals, but Student's t's are more intuitive for understanding the significance, or p-value, of the result.

Complex Network Analyses

Complex network analyses of human whole-brain structural and functional imaging data sets emerged approximately a decade ago (Achard, Salvador, Whitcher, Suckling, & Bullmore, 2006; Bassett, Meyer-Lindenberg, Achard, Duke, & Bullmore, 2006; Eguiluz, Chialvo, Cecchi, Baliki, & Apkarian, 2005; Gong et al., 2009; Hagmann et al., 2008; He, Chen, & Evans, 2007; Iturria-Medina, Sotero, Canales-Rodriguez, Aleman-Gomez, & Melie-Garcia, 2008; Liu et al., 2008; Stam, 2004; Stam, Jones, Nolte, Breakspear, & Scheltens, 2007), in parallel with increasing conceptualization of the brain as a complex network of brain regions and interregional structural and functional associations (Bullmore & Sporns, 2009). Analyses of complex brain networks have coalesced around the notion of the connectome, defined as the complete organizational description of anatomical brain connections (Sporns, 2012; Sporns, Tononi, & Kötter, 2005) and more loosely extended to encompass organizational descriptions of complex brain functional connections, as well descriptions of complex brain connectivity in neurological and psychiatric disorders (Calhoun, Miller, Pearlson, & Adalı, 2014; Kopell, Gritton, Whittington, & Kramer, 2014; Rubinov & Bullmore, 2013).

Complex brain networks represent the organization of whole-brain white-matter pathways, or whole-brain functional coactivation patterns and typically comprise hundreds of brain regions (vertices or nodes) and thousands of interregional connections (edges or links). As a rule of thumb, networks are deemed to be complex if their organization cannot be adequately described with visualizations (Newman, 2010). Complex brain networks contrast with other network models in cognitive neuroscience, which associate with a specific function (such as language), have few nodes, and are easily described with visualizations (Fox & Raichle, 2007).

Accurate definition of nodes in complex brain networks is an important problem, and affects the meaningfulness and interpretability of subsequent network analyses (Rubinov & Sporns, 2010). Nodes should ideally be functionally homogeneous, spatially contiguous, cover the whole-brain, have high signal-to-noise ratio, and be reproducible between subjects (Craddock et al., 2013; Thirion, Varoquaux, Dohmatob, & Poline, 2014). Most current atlases are based on structural (e.g., cytoarchitectonic or transcriptomic) or functional (e.g., regional activity patterns) datasets, but no atlas simultaneously fulfils all the above criteria. High resolution structural or functional imaging may allow the appearance of such gold-standard reference atlases in the next couple of decades (Amunts et al., 2013; Insel, Landis, & Collins, 2013).

Accurate definition of structural or functional brain connections is likewise an important problem, with similar implications for meaningfulness and interpretability. Anatomical connections typically represent white-matter tracts and are inferred with diffusion MRI and tractography or less directly with gray-matter-thickness covariance methods (Alexander-Bloch, Giedd, & Bullmore, 2013; Behrens & Sporns, 2012; Evans, 2013; Hagmann et al., 2010). Functional connections reflect patterns of statistical associations, irrespective of underlying anatomical connectivity, and are inferred with statistical measures such as the Pearson or partial correlation coefficients, mutual information, and lag-based measures such as Granger causality (Smith et al., 2011; Van Dijk et al., 2010). Bayesian network inference methods are used infrequently due to large network sizes, although methodological and computational progress may make these methods more relevant in the future (Seghier & Friston, 2013). Connections may have additional properties of directionality (afferent or efferent), weight (strong or weak), and sign (positive or negative) (Rubinov & Sporns, 2011).

Analysis of complex brain networks leverage methods which have origins in graph-theoretical analyses of social networks, but have been extensively and inter-disciplinarily expanded in the last two decades to describe properties of complex real-life systems in diverse scientific fields (Boccaletti, Latora, Moreno, Chavez, & Hwang, 2006; Newman, 2003). Broadly, such analyses are divided into analyses of global, intermediate or local network organization. Analyses of global organization describe properties of the whole network, analyses of intermediate network organization describe properties of groups of nodes in the network, and analyses of local network organization describe properties of individual nodes.

Analyses of global network organization typically describe the propensity for whole-brain functional specialization and functional integration. Functional specialization is inferred as the extent to which network nodes form clusters and is computed with measures such as the clustering coefficient (the average number of triangles as a fraction of all connected

https://doi.org/10.1017/S1355617716000060 Published online by Cambridge University Press

triplets). Functional integration is measured as the propensity of the network for global interconnectedness and is computed with measures such as the characteristic path length (the average length of shortest paths between all pairs of nodes). The simultaneous presence of functional specialization and integration (relative to random control networks) defines a measure of small-world-ness, a non-specific marker of complex brain network organization (Bassett & Bullmore, 2006; Humphries & Gurney, 2008; Watts & Strogatz, 1998).

Analyses of intermediate network organization typically partition the network into communities or modules, functionally specialized and densely interconnected groups of nodes, and are conceptually similar to independent components analysis (see below) and other clustering methods (Girvan & Newman, 2002; Meunier, Lambiotte, & Bullmore, 2010). Analyses of intermediate network organization may also bipartition the network into a central and dense group of "core" or "rich-club" nodes and a sparsely interconnected group of peripheral nodes (Colizza, Flammini, Serrano, & Vespignani, 2006; van den Heuvel & Sporns, 2011). Importantly, unlike global and local measures of complex network organization, detection of community (and to a lesser extent core-periphery) structure often involves the use of non-deterministic optimization algorithms which may produce many possible solutions (Csermely, London, Wu, & Uzzi, 2013; Fortunato, 2010).

Analyses of local network organization typically quantify the importance of individual nodes in the network. Importance is a subjective notion, but is most commonly defined using measures such as degree (the total number of nodal connections), participation coefficient (the diversity of nodal connections), and the betweenness centrality (fractions of all shortest path traversing the node). The robust detection of hub nodes is a notable strength of complex network analysis and such hubs are increasingly implicated in diverse neurological and psychiatric disorders (Crossley et al., 2014; Harrington et al., 2015; Stam, 2014; van den Heuvel & Sporns, 2013).

The combined global, intermediate and local analyses of complex brain networks provide a comprehensive statistical description of structural and functional organization of the human brain. Inevitably, however, the quality and interpretation of such descriptions relies on the quality of the underlying brain imaging and on adequate definitions of nodes and connections. Increasing spatial and temporal resolution of human imaging is likely to move the analysis and interpretation of complex brain networks closer to biological processes underlying normal and abnormal brain structure, activity and function.

Independent Components Analysis (ICA)

ICA is a statistical method used to discover hidden factors (sources or features) from a set of measurements or observed data such that the sources are maximally independent. Within the context of neuroimaging, the algorithm has been widely implemented on EEG data, identifying independent time courses (for a review, see Eichele, Calhoun, & Debener, 2009; Makeig, Debener, Onton, & Delorme, 2004) or on fMRI data, emphasizing independent spatial maps (for a review, see Calhoun & Adali, 2012). We focus here on fMRI, where ICA reduces the original (voxels × time) observations into a linear mixture of spatially independent brain maps (components) and associated time courses (mixing matrix).

Since the model identifies latent fMRI sources whose voxels have the same time course, each component can be considered a measure of the degree to which each voxel is functionally connected (or correlated) to the component time course. These correlated patterns of activity likely result from activity within somewhat distinct brain modes or sources, which motivates their description as distinct brain networks with potentially distinct properties. For example, the statistical maps generated from cognitive tasks with general linear modeling (GLM) resemble fMRI source maps, even when derived from data collected in the absence of an explicit task (Calhoun & Allen, 2013; Calhoun, Kiehl, & Pearlson, 2008; Smith et al., 2009).

The fMRI source spatial profile depends in part on the model order (i.e., the number of components estimated), with higher model orders resulting in a more detailed parcellation of distinct areas (Abou-Elseoud et al., 2010; Allen et al., 2011). Spatial maps also depend on the particular algorithm implemented in the ICA decomposition (for details on ICA algorithms see Hyvarinen, Karhunen, & Oja, 2001; Stone, 2004). For example, the Infomax algorithm can emphasize sparse independent fMRI maps, which aligns with the assumption of sparse and distributed cognitive activations, and the sparse and spatially specific artifacts that result from motion and cardiac activity (McKeown et al., 1998).

While there is considerable utility in conducting ICA at the subject level, it is difficult to identify common sources across subjects when performing the subsequent group analysis. To address this problem, extensions have been developed to incorporate information from multiple subjects within a single ICA decomposition (Beckmann & Smith, 2005; Calhoun & Adali, 2012; Calhoun, Adali, Pearlson, & Pekar, 2001; Esposito et al., 2005; Guo & Pagnoni, 2008; Schmithorst & Holland, 2004), as implemented within GIFT Matlab software (http://mialab.mrn.org/software/gift) and in MELODIC software (http://www.fmrib.ox.ac.uk/fsl/). Following group ICA, individual subject time courses may be derived by back-reconstructing the group components onto the individual subject data, generating subject specific images and time courses for each component (Calhoun et al., 2001; Erhardt et al., 2011).

While ICA provides a useful data-driven decomposition of functionally distinct networks, many cognitive processes emerge from the collective activity of multiple brain networks (Siegel, Donner, & Engel, 2012; Varela, Lachaux, Rodriguez, & Martinerie, 2001). Thus, there is considerable motivation in examining network interactions *via* associations among the time courses of networks derived from ICA. These interactions are revealed in part by examining cross-correlations between network or component

https://doi.org/10.1017/S1355617716000060 Published online by Cambridge University Press

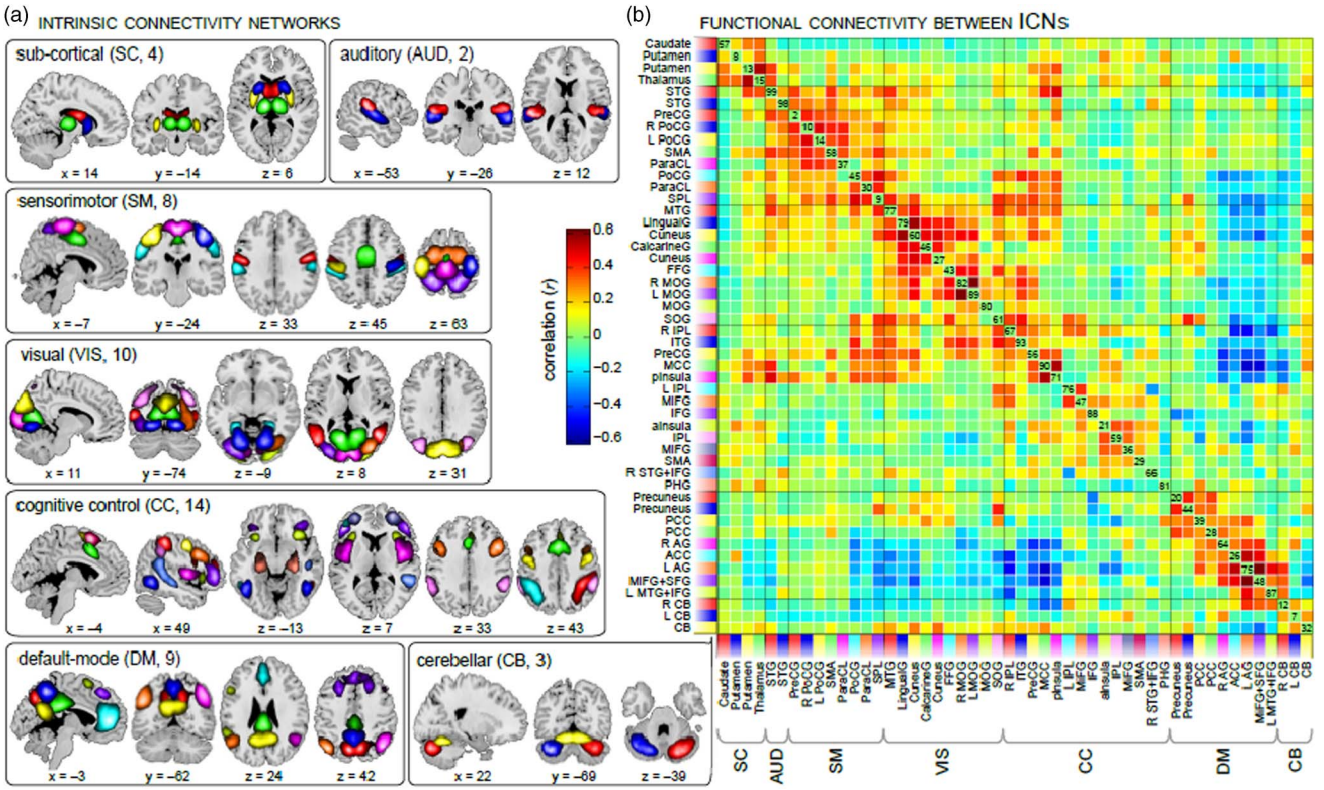


Fig. 2. Examples of within and among network connectivity information. The left panel shows brain regions parcellated from resting fMRI data using group ICA and the right panel shows the functional network connectivity matrix among these regions (cross-correlation).

time courses, resulting in a (component × component) cross-correlation matrix which represents the degree of associations among networks, or the *functional network connectivity (FNC)* (Jafri, Pearlson, Stevens, & Calhoun, 2008). Group ICA is an important processing step within FNC analysis, since it reduces the original (voxels × voxels) cross-correlation matrix into a more tangible (components × components) matrix that compares the relationship between the individual back-reconstructed time courses (see Figure 2).

Cross-correlations are examined either across the entire component time course, revealing static or aggregate measures of connectivity, or within shorter segments, revealing time-varying changes in dynamic FNC (Allen et al., 2014; Chang & Glover, 2010; Sakoğlu et al., 2010). Static connectivity provides an approximate measure of functional associations across the entire time course, but is insensitive to dynamic changes in connectivity patterns which may emerge at shorter time scales (for a review, see Hutchison et al., 2013). Thus, FNC matrices may be calculated from successive ~40- to 60-s intervals and partitioned into groups of recurring connectivity patterns using multivariate approaches such as k-means clustering (Allen et al., 2014; Damaraju et al., 2014; Rashid, Damaraju, Pearlson, & Calhoun, 2014; Sakoğlu et al., 2010), ICA (Yaesoubi, Miller, & Calhoun, 2015) or singular value decomposition (svd) (Leonardi, Shirer, Greicius, & Van De Ville, 2014). Many of these approaches implicitly assume that there are a handful of distinct connectivity patterns (i.e., states), that a single state is present at any given time, and that states recur over minute-to-minute intervals. It will be important for future research to evaluate these assumptions. For example, a recent study suggests that dynamic FNC patterns were better described by overlapping states during rest, but by distinct states during tasks (i.e., silently counting, singing, or recalling events) (Leonardi et al., 2014).

Dynamic FNC analysis may compliment static FNC measures, each capturing different characteristics of network dynamics. For example, while static FNC provides an aggregate measure of connectivity, dFNC provides a parcellation into distinct states which can be characterized by the frequency and duration of occurrence (Calhoun et al., 2014). For example, individuals diagnosed with schizophrenia demonstrate a reduced presence of network connectivity states comprised of large-scale connectivity patterns. These patterns are characterized by increased connectivity among and across visual and somatosensory areas, and decreased connectivity among those regions and regions implicated in cognitive control, that is, the supramarginal gyrus, precuneus, middle frontal gyrus, inferior frontal gyrus, cingulate gyrus, and inferior parietal lobule (Damaraju et al., 2014).

These dynamics were obscured when comparing static connectivity differences between these patients and controls. The reduction of large-scale connectivity within schizophrenia could potentially underlie many symptoms, including the attention and perceptual deficits associated with

https://doi.org/10.1017/S1355617716000060 Published online by Cambridge University Press

the disorder (for a review, see Heinrichs & Zakzanis, 1998; Mesholam-Gately, Giuliano, Goff, Faraone, & Seidman, 2009). Thus, there is considerable utility in examining static and dynamic FNC among group ICA time courses and it will be important for further research to examine the correspondence between these patterns and distinct cognitive processes (Calhoun et al., 2014).

dMRI

Maps of whole-brain anatomic connectomes have been proposed to assess whole-brain patterns of connectivity (Hagmann et al., 2007). The anatomic connectomes demonstrate consistency in terms of scan-rescan reproducibility, correlation with resting-state functional connectivity, and bilateral symmetry. However, these anatomic connectomes likely leave out several important connections, particularly those that traverse fiber crossings, for example, transcallosal connections between hand regions in motor cortex (Hagmann et al., 2008).

An important open question is the definition of anatomic connectivity. Fiber counts from streamline tractography are commonly used to represent anatomic connectivity. However, every tractography algorithm depends on several adjustable parameters. A slight adjustment of any of these can drastically change the fiber count. Measures of tissue integrity along a pathway can be used as an alternative to fiber counts and have been found to relate favorably to functional connectivity (Lowe et al., 2014). Tract-based spatial statistics (TBSS) (Smith et al., 2006) adopts the latter approach to assess tissue injury, but does not use tractography to identify white matter fascicles. Rather, a scalar fractional anisotropy map is used in conjunction with an atlas to identify the fascicles, completely avoiding the algorithmic instabilities associated with tractography. However, the regions identified by TBSS do not directly relate to cortical regions. More recent work involving the TRActs Constrained by UnderLying Anatomy (TRACULA) software (Yendiki et al., 2011) involves a registration-based approach, but constrains analysis to a limited set of well-defined and reliable pathways, thus representing only a small fraction of the total pathways in the brain.

ACKNOWLEDGMENTS

We thank Sally Durgerian for her technical assistance. M.J.L. was supported by the National Multiple Sclerosis Society (RG4931A1/1), NIH (U01NS082083, U01NSN082329, R01NS073717, R01NS035929, R03NS091753), and Genzyme; KES was supported by the American heart Association (13BGIA17120055), NIH P50NS038667, U01NS082329, U01NS082083), National Multiple Sclerosis Society (RG4931A1/1), Novartis, and Genzyme; VDC was supported by NIH (P20GM103472, R01EB006841); MR was supported by the NARSAD Young Investigator Award and the Isaac Newton Grant for Research Purposes; and SMR was supported by NIH (RO1NS040068, U01NS082083, R01NS054893), U.S. Department of Defense (W81XWH-10-1-0609), and CHDI Foundation. The content is solely the responsibility of the authors and does not necessarily represent the official views of the NIH. *Conflicts of Interest:* The authors do not report conflicts of interest related to this manuscript.

REFERENCES

Abou-Elseoud, A., Starck, T., Remes, J., Nikkinen, J., Tervonen, O., & Kiviniemi, V. (2010). The effect of model order selection in group PICA. *Human Brain Mapping*, *31*, 1207–1216.

Achard, S., Salvador, R., Whitcher, B., Suckling, J., & Bullmore, E. (2006). A resilient, low-frequency, small-world human brain functional network with highly connected association cortical hubs. *The Journal of Neuroscience*, *26*(1), 63–72.

Alexander-Bloch, A., Giedd, J.N., & Bullmore, E. (2013). Imaging structural co-variance between human brain regions. [Review]. *Nature Reviews Neuroscience*, *14*(5), 322–336.

Allen, E.A., Damaraju, E., Plis, S.M., Erhardt, E.B., Eichele, T., & Calhoun, V.D. (2014). Tracking Whole-brain connectivity dynamics in the resting state. *Cerebral Cortex*, *24*(3), 663–676.

Allen, E.A., Erhardt, E.B., Damaraju, E., Gruner, W., Segall, J.M., Silva, R.F., … Calhoun, V.D. (2011). A baseline for the multivariate comparison of resting-state networks. *Frontiers in Systems Neuroscience*, *5*, 2.

Amunts, K., Lepage, C., Borgeat, L., Mohlberg, H., Dickscheid, T., Rousseau, M.-É., … Evans, A.C. (2013). BigBrain: An ultrahigh-resolution 3D human brain model. *Science*, *340*(6139), 1472–1475.

Assaf, Y., Blumenfeld-Katzir, T., Yovel, Y., & Basser, P.J. (2008). AxCaliber: A method for measuring axon diameter distribution from diffusion MRI. *Magnetic Resonance in Medicine*, *59*(6), 1347–1354.

Assemlal, H.E., Tschumperle, D., Brun, L., & Siddiqi, K. (2011). Recent advances in diffusion MRI modeling: Angular and radial reconstruction. *Medical Image Analysis*, *15*(4), 369–396.

Barazany, D., Basser, P.J., & Assaf, Y. (2009). In vivo measurement of axon diameter distribution in the corpus callosum of rat brain. *Brain*, *132*(Pt 5), 1210–1220.

Basser, P.J., Mattiello, J., & LeBihan, D. (1994). MR diffusion tensor spectroscopy and imaging. *Biophysical Journal*, *66*(1), 259–267.

Basser, P.J., Pajevic, S., Pierpaoli, C., Duda, J., & Aldroubi, A. (2000). In vivo fiber tractography using DT-MRI data. *Magnetic Resonance in Medicine*, *44*(4), 625–632.

Bassett, D.S., & Bullmore, E. (2006). Small-world brain networks. *Neuroscientist*, *12*(6), 512–523.

Bassett, D.S., Meyer-Lindenberg, A., Achard, S., Duke, T., & Bullmore, E. (2006). Adaptive reconfiguration of fractal small-world human brain functional networks. *Proceedings of the National Academy of Sciences of the United States of America*, *103*(51), 19518–19523.

Beall, E.B., & Lowe, M.J. (2007). Isolating physiologic noise sources with independently determined spatial measures. *Neuroimage*, *37*(4), 1286–1300.

Beall, E.B., & Lowe, M.J. (2010). The non-separability of physiologic noise in functional connectivity MRI with spatial ICA at 3T. *Journal of Neuroscience Methods*, *191*(2), 263–276.

Beall, E.B., & Lowe, M.J. (2014). SimPACE: Generating simulated motion corrupted BOLD data with synthetic-navigated acquisition for the development and evaluation of SLOMOCO: A new, highly effective slicewise motion correction. *Neuroimage*, *101*, 21–34.

https://doi.org/10.1017/S1355617716000060 Published online by Cambridge University Press

Beckmann, C.F., & Smith, S.M. (2005). Tensorial extensions of independent component analysis for multisubject FMRI analysis. *Neuroimage*, *25*(1), 294–311.

Behrens, T.E., Berg, H.J., Jbabdi, S., Rushworth, M.F., & Woolrich, M.W. (2007). Probabilistic diffusion tractography with multiple fibre orientations: What can we gain? *Neuroimage*, *34*(1), 144–155.

Behrens, T.E., & Sporns, O. (2012). Human connectomics. *Current Opinion in Neurobiology*, *22*(1), 144–153.

Bendat, J.S., & Piersol, A.G. (2000). *Random data. Analysis and measurement procedures* (3rd ed.). New York: John Wiley & Sons.

Biswal, B.B., & Hudetz, A.G. (1996). Synchronous oscillations in cerebrocortical capillary red blood cell velocity after nitric oxide synthase inhibition. *Microvascular Research*, *52*(1), 1–12.

Biswal, B.B., Hudetz, A.G., Yetkin, F.Z., Haughton, V.M., & Hyde, J.S. (1997). Hypercapnia reversibly suppresses low-frequency fluctuations in the human motor cortex during rest using echo-planar MRI. *Journal of Cerebral Blood Flow & Metabolism*, *17*(3), 301–308.

Biswal, B.B., Van Kylen, J., & Hyde, J.S. (1997). Simultaneous assessment of flow and BOLD signals in resting-state. *NMR in Biomedicine*, *10*(4-5), 165–170.

Biswal, B.B., Yetkin, F.Z., Haughton, V.M., & Hyde, J.S. (1995). Functional connectivity in the motor cortex of resting human brain. *Magnetic Resonance in Medicine*, *34*(4), 537–541.

Boccaletti, S., Latora, V., Moreno, Y., Chavez, M., & Hwang, D.U. (2006). Complex networks: Structure and dynamics. *Physics Reports*, *424*(4–5), 175–308.

Boubela, R.N., Kalcher, K., Huf, W., Kronnerwetter, C., Filzmoser, P., & Moser, E. (2013). Beyond noise: Using temporal ICA to extract meaningful information from high-frequency fMRI signal fluctuations during rest. *Frontiers in Human Neuroscience*, *7*, 168.

Brookes, M.J., Hale, J.R., Zumer, J.M., Stevenson, C.M., Francis, S.T., Barnes, G.R., … Nagarajan, S.S. (2011). Measuring functional connectivity using MEG: Methodology and comparison with fcMRI. *Neuroimage*, *56*(3), 1082–1104.

Budde, M.D., Kim, J.H., Liang, H.F., Schmidt, R.E., Russell, J.H., Cross, A.H., & Song, S.K. (2007). Toward accurate diagnosis of white matter pathology using diffusion tensor imaging. *Magnetic Resonance in Medicine*, *57*(4), 688–695.

Bullmore, E.T., Brammer, M.J., Rabe-Hesketh, S., Curtis, V.A., Morris, R.G., Williams, S.C., … McGuire, P.K. (1999). Methods for diagnosis and treatment of stimulus-correlated motion in generic brain activation studies using fMRI. *Human Brain Mapping*, *7*(1), 38–48.

Bullmore, E.T., & Sporns, O. (2009). Complex brain networks: Graph theoretical analysis of structural and functional systems. *Nature Reviews Neuroscience*, *10*(3), 186–198.

Buzsaki, G. (2006). *Rhythms of the brain*. New York: Oxford University Press.

Calhoun, V.D., & Adali, T. (2012). Multi-subject independent component analysis of fMRI: A decade of intrinsic networks, default mode, and neurodiagnostic discovery. *IEEE Reviews in Biomedical Engineering*, *5*, 60–72.

Calhoun, V.D., Adali, T., Pearlson, G.D., & Pekar, J.J. (2001). A method for making group inferences from functional MRI data using independent component analysis. *Human Brain Mapping*, *14*(3), 140–151.

Calhoun, V.D., & Allen, E. (2013). Extracting intrinsic functional networks with feature-based group independent component analysis. *Psychometrika*, *78*(2), 243–259.

Calhoun, V.D., Kiehl, K.A., & Pearlson, G.D. (2008). Modulation of temporally coherent brain networks estimated using ICA at rest and during cognitive tasks. *Human Brain Mapping*, *29*(7), 828–838.

Calhoun, V.D., Miller, R., Pearlson, G., & Adalı, T. (2014). The chronnectome: Time-varying connectivity networks as the next frontier in fMRI data discovery. *Neuron*, *84*(2), 262–274.

Catani, M., Howard, R.J., Pajevic, S., & Jones, D.K. (2002). Virtual in vivo interactive dissection of white matter fasciculi in the human brain. *Neuroimage*, *17*(1), 77–94.

Chang, C., & Glover, G.H. (2010). Time–frequency dynamics of resting-state brain connectivity measured with fMRI. *Neuroimage*, *50*(1), 81–98.

Cohen, D., & Cuffin, B.N. (1983). Demonstration of useful differences between magnetoencephalogram and electroencephalogram. *Electroencephalography and Clinical Neurophysiology*, *56*(1), 38–51.

Cole, D.M., Smith, S.M., & Beckmann, C.F. (2010). Advances and pitfalls in the analysis and interpretation of resting-state FMRI data. *Frontiers in Systems Neuroscience*, *4*, 8.

Colizza, V., Flammini, A., Serrano, M.A., & Vespignani, A. (2006). Detecting rich-club ordering in complex networks. [10.1038/nphys209]. *Nature Physics*, *2*(2), 110–115.

Conturo, T.E., Lori, N.F., Cull, T.S., Akbudak, E., Snyder, A.Z., Shimony, J.S., … Raichle, M.E. (1999). Tracking neuronal fiber pathways in the living human brain. *Proceedings of the National Academy of Sciences of the United States of America*, *96*(18), 10422–10427.

Cooper, R., Crow, H.J., Walter, W.G., & Winter, A.L. (1966). Regional control of cerebral vascular reactivity and oxygen supply in man. *Brain Research*, *3*(2), 174–191.

Cordes, D., Haughton, V.M., Arfanakis, K., Carew, J.D., Turski, P.A., Moritz, C.H., … Meyerand, M.E. (2001). Frequencies contributing to functional connectivity in the cerebral cortex in "resting-state" data. *AJNR American Journal of Neuroradiology*, *22*(7), 1326–1333.

Cordes, D., Haughton, V.M., Arfanakis, K., Wendt, G.J., Turski, P.A., Moritz, C.H., … Meyerand, M.E. (2000). Mapping functionally related regions of brain with functional connectivity MR imaging. *AJNR American Journal of Neuroradiology*, *21*(9), 1636–1644.

Cordes, D., Nandy, R.R., Schafer, S., & Wager, T.D. (2014). Characterization and reduction of cardiac- and respiratory-induced noise as a function of the sampling rate (TR) in fMRI. *Neuroimage*, *89*, 314–330.

Cox, R.W. (1996). AFNI: Software for analysis and visualization of functional magnetic resonance neuroimages. *Computers and Biomedical Research*, *29*(3), 162–173.

Craddock, R.C., Jbabdi, S., Yan, C.-G., Vogelstein, J.T., Castellanos, F.X., Di Martino, A., … Milham, M.P. (2013). Imaging human connectomes at the macroscale. *Nature Methods*, *10*(6), 524–539.

Crossley, N.A., Mechelli, A., Scott, J., Carletti, F., Fox, P.T., McGuire, P., & Bullmore, E.T. (2014). The hubs of the human connectome are generally implicated in the anatomy of brain disorders. *Brain*, *137*(Pt 8), 2382–2395.

Csermely, P., London, A., Wu, L.-Y., & Uzzi, B. (2013). Structure and dynamics of core/periphery networks. *Journal of Complex Networks*, *1*(2), 93–123.

Damaraju, E., Allen, E.A., Belger, A., Ford, J.M., McEwen, S., Mathalon, D.H., … Calhoun, V.D. (2014). Dynamic functional connectivity analysis reveals transient states of dysconnectivity in schizophrenia. *Neuroimage. Clinical*, *5*, 298–308.

https://doi.org/10.1017/S1355617716000060 Published online by Cambridge University Press

Dora, E., & Kovach, A.G. (1981). Metabolic and vascular volume oscillations in the cat brain cortex. *Acta Physiology of the Academy of Science of Hungary*, *57*(3), 261–275.

Douaud, G., Jbabdi, S., Behrens, T.E., Menke, R.A., Gass, A., Monsch, A.U., … Smith, S. (2011). DTI measures in crossing-fibre areas: Increased diffusion anisotropy reveals early white matter alteration in MCI and mild Alzheimer's disease. *Neuroimage*, *55*(3), 880–890.

Eguiluz, V.M., Chialvo, D.R., Cecchi, G.A., Baliki, M., & Apkarian, A.V. (2005). Scale-free brain functional networks. *Physical Review Letters*, *94*(1), 018102.

Eichele, T., Calhoun, V.D., & Debener, S. (2009). Mining EEG–fMRI using independent component analysis. *International Journal of Psychophysiology*, *73*(1), 53–61.

Engel, A.K., Fries, P., & Singer, W. (2001). Dynamic predictions: Oscillations and synchrony in top-down processing. *Nature Reviews Neuroscience*, *2*, 704–716.

Erhardt, E.B., Rachakonda, S., Bedrick, E.J., Allen, E.A., Adali, T., & Calhoun, V.D. (2011). Comparison of multi-subject ICA methods for analysis of fMRI data. *Human Brain Mapping*, *32*(12), 2075–2095.

Esposito, F., Scarabino, T., Hyvarinen, A., Himberg, J., Formisano, E., Comani, S., … Salle, F. (2005). Independent component analysis of fMRI group studies by self-organizing clustering. *Neuroimage*, *25*(1), 193–205.

Evans, A.C. (2013). Networks of anatomical covariance. *Neuroimage*, *80*, 489–504.

Fortunato, S. (2010). Community detection in graphs. *Physics Reports*, *486*(3-5), 75–174.

Fox, M.D., & Raichle, M.E. (2007). Spontaneous fluctuations in brain activity observed with functional magnetic resonance imaging. *Nature Reviews Neuroscience*, *8*(9), 700–711.

Friston, K.J., Frith, C.D., Liddle, P.F., & Frackowiak, R.S. (1993). Functional connectivity: The principal-component analysis of large (PET) data sets. *Journal of Cerebral Blood Flow & Metabolism*, *13*(1), 5–14.

Geschwind, N. (1965a). Disconnexion syndromes in animals and man. I. *Brain*, *88*(2), 237–294.

Geschwind, N. (1965b). Disconnexion syndromes in animals and man. II. *Brain*, *88*(3), 585–644.

Girvan, M., & Newman, M.E.J. (2002). Community structure in social and biological networks. *Proceedings of the National Academy of Sciences of the United States of America*, *99*(12), 7821–7826.

Glover, G.H., Li, T.Q., & Ress, D. (2000). Image-based method for retrospective correction of physiological motion effects in fMRI: RETROICOR. *Magnetic Resonance in Medicine*, *44*(1), 162–167.

Golanov, E.V., Yamamoto, S., & Resi, D.J. (1994). Spontaneous waves of cerebral blood flow associated with patterns of electrocortical activity. *American Journal of Physiology*, *266*, R204–R214.

Gong, G., He, Y., Concha, L., Lebel, C., Gross, D.W., Evans, A.C., & Beaulieu, C. (2009). Mapping anatomical connectivity patterns of human cerebral cortex using in vivo diffusion tensor imaging tractography. *Cerebral Cortex*, *19*(3), 524–536.

Greicius, M.D., Krasnow, B., Reiss, A.L., & Menon, V. (2003). Functional connectivity in the resting brain: A network analysis of the default mode hypothesis. *Proceedings of the National Academy of Sciences of the United States of America*, *100*(1), 253–258.

Guo, Y., & Pagnoni, G. (2008). A unified framework for group independent component analysis for multi-subject fMRI data. *Neuroimage*, *42*(3), 1078–1093.

Gusnard, D.A., Akbudak, E., Shulman, G.L., & Raichle, M.E. (2001). Medial prefrontal cortex and self-referential mental activity: Relation to a default mode of brain function. *Proceedings of the National Academy of Sciences of the United States of America*, *98*(7), 4259–4264.

Hagmann, P., Cammoun, L., Gigandet, X., Gerhard, S., Grant, P.E., Wedeen, V.J., … Sporns, O. (2010). MR connectomics: Principles and challenges. *Journal of Neuroscience Methods*, *194*(1), 34–45.

Hagmann, P., Cammoun, L., Gigandet, X., Meuli, R., Honey, C.J., Wedeen, V.J., & Sporns, O. (2008). Mapping the structural core of human cerebral cortex. *PLoS Biology*, *6*(7), e159.

Hagmann, P., Kurant, M., Gigandet, X., Thiran, P., Wedeen, V.J., Meuli, R., & Thiran, J.P. (2007). Mapping human whole-brain structural networks with diffusion MRI. *PLoS One*, *2*(7), e597.

Halsey, J.H., Jr., & McFarland, S. (1974). Oxygen cycles and metabolic autoregulation. *Stroke*, *5*(2), 219–225.

Harrington, D.L., Rubinov, M., Durgerian, S., Mourany, L., Reece, C., Koenig, K., … Rao, S.M. (2015). Network topology and functional connectivity disturbances precede the onset of Huntington's disease. *Brain*, *138*(Pt 8), 2332–2346.

He, Y., Chen, Z.J., & Evans, A.C. (2007). Small-world anatomical networks in the human brain revealed by cortical thickness from MRI. *Cerebral Cortex*, *17*(10), 2407–2419.

Heinrichs, H.R., & Zakzanis, K.K. (1998). Neurocognitive deficit in schizophrenia: A quantitative review of the evidence. *Neuropsychology*, *12*(3), 426–445.

Hudetz, A.G., Smith, J.J., Lee, J.G., Bosnjak, Z.J., & Kampine, J.P. (1995). Modification of cerebral laser-Doppler flow oscillations by halothane, PCO2, and nitric oxide synthase blockade. *American Journal of Physiology*, *269*(1 Pt 2), H114–H120.

Humphries, M.D., & Gurney, K. (2008). Network 'Small-World-Ness': A quantitative method for determining canonical network equivalence. *PLoS One*, *3*(4), e0002051.

Hutchison, R.M., Womelsdorf, T., Allen, E.A., Bandettini, P.A., Calhoun, V.D., Corbetta, M., … Chang, C. (2013). Dynamic functional connectivity: Promise, issues, and interpretations. *Neuroimage*, *80*, 360–378.

Hyvarinen, A., Karhunen, J., & Oja, E. (2001). *Independent component analysis*. New York: John Wiley & Sons.

Insel, T.R., Landis, S.C., & Collins, F.S. (2013). Research priorities. The NIH BRAIN Initiative. *Science*, *340*(6133), 687–688.

Iturria-Medina, Y., Sotero, R.C., Canales-Rodriguez, E.J., Aleman-Gomez, Y., & Melie-Garcia, L. (2008). Studying the human brain anatomical network via diffusion-weighted MRI and Graph Theory. *Neuroimage*, *40*(3), 1064–1076.

Jafri, M.J., Pearlson, G.D., Stevens, M., & Calhoun, V.D. (2008). A method for functional network connectivity among spatially independent resting-state components in schizophrenia. *Neuroimage*, *39*(4), 1666–1681.

Johansen-Berg, H., & Behrens, T.E.J. (2009). *Diffusion MRI: From quantitative measurement to in-vivo neuroanatomy* (1st ed.). Boston: Elsevier/Academic Press.

Jones, D.K. (2004). The effect of gradient sampling schemes on measures derived from diffusion tensor MRI: A Monte Carlo study. *Magnetic Resonance in Medicine*, *51*(4), 807–815.

Jones, D.K. (2010). *Diffusion MRI: Theory, methods, and applications*. New York: Oxford University Press.

Kalcher, K., Boubela, R.N., Huf, W., Bartova, L., Kronnerwetter, C., Derntl, B., … Moser, E. (2014). The spectral diversity of resting-state fluctuations in the human brain. *PLoS One*, *9*(4), e93375.

https://doi.org/10.1017/S1355617716000060 Published online by Cambridge University Press

Kenet, T., Bibitchkov, D., Tsodyks, M., Grinvald, A., & Arieli, A. (2003). Spontaneously emerging cortical representations of visual attributes. *Nature*, *425*(6961), 954–956.

Kopell, N.J., Gritton, H.J., Whittington, M.A., & Kramer, M.A. (2014). Beyond the connectome: The dynome. *Neuron*, *83*(6), 1319–1328.

Laufs, H., Krakow, K., Sterzer, P., Eger, E., Beyerle, A., Salek-Haddadi, A., & Kleinschmidt, A. (2003). Electroencephalographic signatures of attentional and cognitive default modes in spontaneous brain activity fluctuations at rest. *Proceedings of the National Academy of Sciences of the United States of America*, *100*(19), 11053–11058.

Leonardi, N., Shirer, W.R., Greicius, l.D., & Van De Ville, D. (2014). Disentangling dynamic networks: Separated and joint expressions of functional connectivity patterns in time: Disentangling dynamic networks. *Human Brain Mapping*, *35*(12), 5984–5995.

Leopold, D.A., Murayama, Y., & Logothetis, N.K. (2003). Very slow activity fluctuations in monkey visual cortex: Implications for functional brain imaging. *Cerebral Cortex*, *13*(4), 422–433.

Liu, Y., Liang, M., Zhou, Y., He, Y., Hao, Y., Song, M., … Jiang, T. (2008). Disrupted small-world networks in schiz + ophrenia. *Brain*, *131*(Pt 4), 945–961.

Logothetis, N.K. (2002). The neural basis of the blood-oxygen-level-dependent functional magnetic resonance imaging signal. *Philosophical Transactions of the Royal Society B: Biological Sciences*, *357*(1424), 1003–1037.

Logothetis, N.K., Pauls, J., Augath, M., Trinath, T., & Oeltermann, A. (2001). Neurophysiological investigation of the basis of the fMRI signal. *Nature*, *412*(6843), 150–157.

Lowe, M.J., Beall, E.B., Sakaie, K.E., Koenig, K.A., Stone, L., Marrie, R.A., & Phillips, M.D. (2008). Resting state sensorimotor functional connectivity in multiple sclerosis inversely correlates with transcallosal motor pathway transverse diffusivity. *Human Brain Mapping*, *29*(7), 818–827.

Lowe, M.J., Dzemidzic, M., Lurito, J.T., Mathews, V.P., & Phillips, M.D. (2000). Correlations in low-frequency BOLD fluctuations reflect cortico-cortical connections. *Neuroimage*, *12*(5), 582–587.

Lowe, M.J., Horenstein, C., Hirsch, J.G., Marrie, R.A., Stone, L., Bhattacharyya, P.K., *et al*. (2006). Functional pathway-defined MRI diffusion measures reveal increased transverse diffusivity of water in multiple sclerosis. *Neuroimage*, *32*(3), 1127–1133.

Lowe, M.J., Koenig, K.A., Beall, E.B., Sakaie, K., Stone, L., Bermel, R., & Phillips, M.D. (2014). Anatomic connectivity assessed using pathway radial diffusivity is related to functional connectivity in monosynaptic pathways. *Brain Connectivity*, *4*(7), 558–565.

Lowe, M.J., Mock, B.J., & Sorenson, J.A. (1998). Functional connectivity in single and multislice echoplanar imaging using resting-state fluctuations. *Neuroimage*, *7*(2), 119–132.

Lowe, M.J., & & Russell, D.P. (1999). Treatment of baseline drifts in fMRI time series analysis. *Journal of Computer Assisted Tomography*, *23*(3), 463–473.

Lowe, M.J., Rutecki, P., Woodard, A., Turski, P., & Sorenson, J.A. (1997). Auditory cortex fMRI noise correlations in callosal agenesis. *Human Brain Mapping*, *5*(4), S194.

Lowe, M.J., & Sorenson, J.A. (1997). Spatially filtering functional magnetic resonance imaging data. *Magnetic Resonance in Medicine*, *37*(5), 723–729.

Makeig, S., Debener, S., Onton, J., & Delorme, A. (2004). Mining event-related brain dynamics. *Trends in Cognitive Sciences*, *8*(5), 204–210.

McKeown, M.J., Makeig, S., Brown, G.G., Jung, T.P., Kindermann, S.S., Bell, A.J., & Sejnowski, T.J. (1998). Analysis of fMRI data by blind separation into independent spatial components. *Human Brain Mapping*, *6*, 160–629.

Mesholam-Gately, R.I., Giuliano, A.J., Goff, K.P., Faraone, S.V., & Seidman, L.J. (2009). Neurocognition in first-episode schizophrenia: A meta-analytic review. *Neurophysiology*, *23*(3), 315–336.

Meunier, D., Lambiotte, R., & Bullmore, E.T. (2010). Modular and hierarchically modular organization of brain networks. *Frontiers in Neuroscience*, *4*, 200.

Michel, C.M., Murray, M.M., Lantz, G., Gonzalez, S., Spinelli, L., & Grave de Peralta, R. (2004). EEG source imaging. *Clinical Neurophysiology*, *115*(10), 2195–2222.

Mori, S., Crain, B.J., Chacko, V.P., & van Zijl, P.C. (1999). Three-dimensional tracking of axonal projections in the brain by magnetic resonance imaging. *Annals of Neurology*, *45*(2), 265–269.

Moskalenko, Y.E. (1980). *Biophysical aspects of cerebral circulation*. Oxford: Pergamon Press.

Newman, M. (2003). The structure and function of complex networks. *SIAM Review*, *45*(2), 167–256.

Newman, M. (2010). *Networks: An introduction*. Oxford: Oxford University Press.

Nunez, P.L., Silberstein, R.B., Shi, Z., Carpenter, M.R., Srinivasan, R., Tucker, D.M., … Wijesinghe, R.S. (1999). EEG coherency II: Experimental comparisons of multiple measures. *Clinical Neurophysiology*, *110*(3), 469–486.

Nunez, P.L., & Srinivasan, R. (2006). *Electric fields of the brain: The neurophysics of EEG* (2nd ed.). New York: Oxford University Press.

Nunez, P.L., Srinivasan, R., Westdorp, A.F., Wijesinghe, R.S., Tucker, D.M., Silberstein, R. B., & Cadusch, P. J. (1997). EEG coherency: I: Statistics, reference electrode, volume conduction, Laplacians, cortical imaging, and interpretation at multiple scales. *Electroencephalography and Clinical Neurophysiology*, *103*(5), 499–515.

Obrig, H., Neufang, M., Wenzel, R., Kohl, M., Steinbrink, J., Einhaupl, K., *et al*. (2000). Spontaneous low frequency oscillations of cerebral hemodynamics and metabolism in human adults. *Neuroimage*, *12*(6), 623–639.

Oguz, I., Farzinfar, M., Matsui, J., Budin, F., Liu, Z., Gerig, G., … Styner, M. (2014). DTIPrep: Quality control of diffusion-weighted images. *Frontiers in Neuroinformatics*, *8*, 4.

Peltier, S.J., & Noll, D.C. (2002). T(2)(*) dependence of low frequency functional connectivity. *Neuroimage*, *16*(4), 985–992.

Perlbarg, V., Bellec, P., Anton, J.L., Pelegrini-Issac, M., Doyon, J., & Benali, H. (2007). CORSICA: Correction of structured noise in fMRI by automatic identification of ICA components. *Magnetic Resonance Imaging*, *25*(1), 35–46.

Pierpaoli, C., Barnett, A., Pajevic, S., Chen, R., Penix, L.R., Virta, A., & Basser, P. (2001). Water diffusion changes in Wallerian degeneration and their dependence on white matter architecture. *Neuroimage*, *13*(6 Pt 1), 1174–1185.

Power, J.D., Mitra, A., Laumann, T.O., Snyder, A.Z., Schlaggar, B. L., & Petersen, S.E. (2012). Methods to detect, characterize, and remove motion artifact in resting state fMRI. *Neuroimage*, *84C*, 320–341.

Power, J.D., Schlaggar, B.L., & Petersen, S.E. (2015). Recent progress and outstanding issues in motion correction in resting state fMRI. *Neuroimage*, *105*, 536–551.

https://doi.org/10.1017/S1355617716000060 Published online by Cambridge University Press

Press, W., Teukolsky, S., Vetterling, W., & Flannery, B. (1993). *Numerical recipes in C: The art of scientific computing*. Cambridge: Cambridge University Press.

Pruim, R.H., Mennes, M., Buitelaar, J.K., & Beckmann, C.F. (2015). Evaluation of ICA-AROMA and alternative strategies for motion artifact removal in resting state fMRI. *Neuroimage*, *112*, 278–287.

Quigley, M., Cordes, D., Turski, P., Moritz, C., Haughton, V., Seth, R., & Meyerand, M.E. (2003). Role of the corpus callosum in functional connectivity. *AJNR American Journal of Neuroradiology*, *24*(2), 208–212.

Raichle, M.E., MacLeod, A. M., Snyder, A. Z., Powers, W.J., Gusnard, D.A., & Shulman, G.L. (2001). A default mode of brain function. *Proceedings of the National Academy of Sciences of the United States of America*, *98*(2), 676–682.

Rashid, B., Damaraju, E., Pearlson, G.D., & Calhoun, V.D. (2014). Dynamic connectivity states estimated from resting fMRI Identify differences among Schizophrenia, bipolar disorder, and healthy control subjects. *Frontiers in Human Neuroscience*, *8*, 897.

Rubinov, M., & Bullmore, E. (2013). Fledgling pathoconnectomics of psychiatric disorders. *Trends in Cognitive Sciences*, *17*(12), 641–647.

Rubinov, M., & Sporns, O. (2010). Complex network measures of brain connectivity: Uses and interpretations. *Neuroimage*, *52*(3), 1059–1069.

Rubinov, M., & Sporns, O. (2011). Weight-conserving characterization of complex functional brain networks. *Neuroimage*, *56*(4), 2068–2079.

Sakoğlu, Ü., Pearlson, G.D., Kiehl, K.A., Wang, Y.M., Michael, A. M., & Calhoun, V.D. (2010). A method for evaluating dynamic functional network connectivity and task-modulation: Application to schizophrenia. *Magnetic Resonance Materials in Physics, Biology and Medicine*, *23*(5-6), 351–366.

Schmithorst, V.J., & Holland, S.K. (2004). Comparison of three methods for generating group statistical inferences from independent component analysis of functional magnetic resonance imaging data. *Journal of Magnetic Resonance Imaging*, *19*(3), 365–368.

Schoffelen, J.-M., & Gross, J. (2009). Source connectivity analysis with MEG and EEG. *Human Brain Mapping*, *30*(6), 1857–1865.

Seghier, M.L., & Friston, K.J. (2013). Network discovery with large DCMs. *Neuroimage*, *68*(C), 181–191.

Siegel, M., Donner, T.H., & Engel, A.K. (2012). Spectral fingerprints of large-scale neuronal interactions. *Nature Reviews Neuroscience*, *12*, 121–134.

Skare, S., & Andersson, J.L. (2001). On the effects of gating in diffusion imaging of the brain using single shot EPI. *Magnetic Resonance in Medicine*, *19*(8), 1125–1128.

Smith, S.M., Fox, P.T., Miller, K.L., Glahn, D.C., Fox, P.M., Mackay, C.E., … Beckmann, C.F. (2009). Correspondence of the brain's functional architecture during activation and rest. *Proceedings of the National Academy of Sciences of the United States of America*, *106*(31), 13040–13045.

Smith, S.M., Jenkinson, M., Johansen-Berg, H., Rueckert, D., Nichols, T.E., Mackay, C.E., … Behrens, T.E. (2006). Tract-based spatial statistics: Voxelwise analysis of multi-subject diffusion data. *Neuroimage*, *31*(4), 1487–1505.

Smith, S.M., Miller, K.L., Salimi-Khorshidi, G., Webster, M., Beckmann, C.F., Nichols, T.E., … Woolrich, M.W. (2011). Network modelling methods for FMRI. *Neuroimage*, *54*(2), 875–891.

Song, S.K., Sun, S.W., Ju, W.K., Lin, S.J., Cross, A.H., & Neufeld, A.H. (2003). Diffusion tensor imaging detects and differentiates axon and myelin degeneration in mouse optic nerve after retinal ischemia. *Neuroimage*, *20*(3), 1714–1722.

Sporns, O. (2012). *Discovering the human connectome*. Cambridge, MA: MIT Press.

Sporns, O., Tononi, G., & Kötter, R. (2005). The human connectome: A structural description of the human brain. *PLoS Computational Biology*, *1*(4), e42.

Srinivasan, R., Winter, W.R., Ding, J., & Nunez, P.L. (2007). EEG and MEG coherence: Measures of functional connectivity at distinct spatial scales of neocortical dynamics. *Journal of Neuroscience Methods*, *166*(1), 41–52.

Stam, C.J. (2004). Functional connectivity patterns of human magnetoencephalographic recordings: A 'small-world' network? *Neuroscience Letters*, *355*(1–2), 25–28.

Stam, C.J. (2014). Modern network science of neurological disorders. [Review]. *Nature Reviews Neuroscience*, *15*(10), 683.

Stam, C.J., Jones, B.F., Nolte, G., Breakspear, M., & Scheltens, P. (2007). Small-world networks and functional connectivity in Alzheimer's disease. *Cerebral Cortex*, *17*(1), 92–99.

Stanisz, G.J., Szafer, A., Wright, G.A., & Henkelman, R.M. (1997). An analytical model of restricted diffusion in bovine optic nerve. *Magnetic Resonance in Medicine*, *37*(1), 103–111.

Stone, J.V. (2004). *Independent component analysis: A tutorial introduction*. Cambridge, MA: MIT press.

Strother, S.C., Anderson, J.R., Schaper, K.A., Sidtis, J.J., Liow, J.S., Woods, R.P., … Rottenberg, D.A. (1995). Principal component analysis and the scaled subprofile model compared to intersubject averaging and statistical parametric mapping: I. "Functional connectivity" of the human motor system studied with [15O] water PET. *Journal of Cerebral Blood Flow & Metabolism*, *15*(5), 738–753.

Thirion, B., Varoquaux, G., Dohmatob, E., & Poline, J.-B. (2014). Which fMRI clustering gives good brain parcellations? [Original Research]. *Frontiers in Neuroscience*, *8*, 167.

Tournier, J.D., Mori, S., & Leemans, A. (2011). Diffusion tensor imaging and beyond. *Magnetic Resonance in Medicine*, *65*(6), 1532–1556.

van den Heuvel, M.P., & Sporns, O. (2011). Rich-club organization of the human connectome. *The Journal of Neuroscience*, *31*(44), 15775–15786.

van den Heuvel, M.P., & Sporns, O. (2013). Network hubs in the human brain. *Trends in Cognitive Sciences*, *17*(12), 683–696.

Van Dijk, K.R., Hedden, T., Venkataraman, A., Evans, K.C., Lazar, S.W., & Buckner, R.L. (2010). Intrinsic functional connectivity as a tool for human connectomics: Theory, properties, and optimization. *Journal of Neurophysiology*, *103*, 297–321.

Varela, F., Lachaux, J.P., Rodriguez, E., & Martinerie, J. (2001). The brainweb: Phase synchronization and large-scale integration. *Nature Reviews. Neuroscience*, *2*(4), 229–239.

Vern, B.A., Schuette, W.H., Leheta, B., Juel, V.C., & Radulovacki, M. (1988). Low-frequency oscillations of cortical oxidative metabolism in waking and sleep. *Journal of Cerebral Blood Flow & Metabolism*, *8*(2), 215–226.

Wang, Y., Wang, Q., Haldar, J.P., Yeh, F.C., Xie, M., Sun, P., … Song, S.K. (2011). Quantification of increased cellularity during inflammatory demyelination. *Brain*, *134*(Pt 12), 3590–3601.

Watts, D.J., & Strogatz, S.H. (1998). Collective dynamics of /"small-world/" networks. *Nature*, *393*(6684), 440–442.

https://doi.org/10.1017/S1355617716000060 Published online by Cambridge University Press

Wheeler-Kingshott, C.A., & Cercignani, M. (2009). About "axial" and "radial" diffusivities. *Magnetic Resonance in Medicine*, *61*(5), 1255–1260.

Yaesoubi, M., Miller, R.L., & Calhoun, V.D. (2015). Mutually temporally independent connectivity patterns: A new framework to study the dynamics of brain connectivity at rest with application to explain group difference based on gender. *Neuroimage*, *107*, 85–94.

Yang, H., Long, X.Y., Yang, Y., Yan, H., Zhu, C.Z., Zhou, X.P., … Gong, Q, Y. (2007). Amplitude of low frequency fluctuation within visual areas revealed by resting-state functional MRI. *Neuroimage*, *36*(1), 144–152.

Yendiki, A., Koldewyn, K., Kakunoori, S., Kanwisher, N., & Fischl, B. (2013). Spurious group differences due to head motion in a diffusion MRI study. *Neuroimage*, *88C*, 79–90.

Yendiki, A., Panneck, P., Srinivasan, P., Stevens, A., Zollei, L., Augustinack, J., … Fischl, B. (2011). Automated probabilistic reconstruction of white-matter pathways in health and disease using an atlas of the underlying anatomy. *Frontiers in Neuroinformatics*, *5*, 23.

Zang, Y., Jiang, T., Lu, Y., He, Y., & Tian, L. (2004). Regional homogeneity approach to fMRI data analysis. *Neuroimage*, *22*(1), 394–400.

https://doi.org/10.1017/S1355617716000060 Published online by Cambridge University Press